HOKKAIDO UNIVERSITY

Title	A mouse model of short-term, diet-induced fatty liver with abnormal cardiolipin remodeling via downregulated Tafazzin gene expression
Author(s)	Sakurai, Toshihiro; Chen, Zhen; Yamahata, Arisa et al.
Citation	Journal of the science of food and agriculture, 101(12), 4995-5001 https://doi.org/10.1002/jsfa.11144
Issue Date	2021-08-05
Doc URL	https://hdl.handle.net/2115/86499
Rights	This is the peer reviewed version of the following article: Sakurai, T., Chen, Z., Yamahata, A., Hayasaka, T., Satoh, H., Sekiguchi, H., Chiba, H., & Hui, S. P. (2021). A mouse model of short-term, diet-induced fatty liver with abnormal cardiolipin remodeling via downregulated Tafazzin gene expression. Journal of the science of food and agriculture, 101(12), 4995-5001, which has been published in final form at https://doi.org/10.1002/jsfa.11144. This article may be used for non-commercial purposes in accordance with Wiley Terms and Conditions for Use of Self-Archived Versions. This article may not be enhanced, enriched or otherwise transformed into a derivative work, without express permission from Wiley or by statutory rights under applicable legislation. Copyright notices must not be removed, obscured or modified. The article must be linked to Wiley's version of record on Wiley Online Library and any embedding, framing or otherwise making available the article or pages thereof by third parties from platforms, services and websites other than Wiley Online Library must be prohibited.
Type	journal article
File Information	20210115_MLCL_Taz_Manuscript_Resubmission_Final ver.pdf

Hokkaido University Collection of Scholarly and Academic Papers : HUSCAP

A mouse model of short-term, diet-induced fatty liver with abnormal cardiolipin remodeling via downregulated Tafazzin gene expression

Toshihiro Sakurai [1,*], Zhen Chen [1,*], Arisa Yamahata [1,*], Takahiro Hayasaka [1], Hiroshi Satoh [2,3], Hirotaka Sekiguchi [2,4], Hitoshi Chiba [5], Shu-Ping Hui [1]

[1] Faculty of Health Sciences, Hokkaido University, Sapporo 060-0812, Japan

[2] Department of Food and Health Research, Life Science Institute Co. Ltd and Nissei Bio Co. Ltd, Center for Food and Medical Innovation, Institute for the Promotion of Business-Regional Collaboration, Hokkaido University, Sapporo, Japan

[3] Research and Development division, Hokkaido Research Institute, Nissei Bio Co. Ltd, Eniwa, Japan

[4] R&D Planning and Administration Department, Life Science Institute Co., Ltd, Tokyo, Japan

[5] Department of Nutrition, Sapporo University of Health Sciences, Sapporo 007-0894, Japan

Correspondence: SP Hui.

Kita 12, Nishi 5, Kita-ku, Sapporo 060-0812, Japan.

E-mail: keino@hs.hokudai.ac.jp

* TS, ZC, and AY contributed equally.

Running title:

A short-term fatty-liver mouse model with abnormal CL remodeling

Abbreviations:

CL, Cardiolipin; MLCL, monolysocardiolipin; HCD, high carbohydrate diet; Taz, Tafazzin; Lclat1, Lysocardiolipin acyltransferase 1; Pnpla8, Calcium-independent phospholipase A2-gamma; Cls, Cardiolipin synthase; NCD, normal chow diet; ESI, electrospray ionization; PG, phosphatidylglycerol.

Keywords: high-carbohydrate diet; liquid chromatography mass spectrometry; lipidomics; mitochondria; monolysocardiolipin.

Abstract

Background: Cardiolipin (CL) helps maintain mitochondrial structure and function. Here we investigated whether a high carbohydrate diet (HCD) fed to mice for a short term (5 days) can modulate the CL level including that of monolysoCL (MLCL) in the liver.

Results: Total CL in the HCD group was 22% lower than that in the normal chow diet (NCD) group (P <0.05). CL72:8 level strikingly decreased by 93% (P <0.0001), whereas total nascent CL (CLs other than CL72:8) increased (P <0.01) in the HCD group. Moreover, total MLCL in the HCD group increased by 2.4-fold compared with that in the NCD group (P <0.05). *Tafazzin* expression in the HCD group was significantly downregulated compared with that in the NCD group (P <0.05). A strong positive correlation between nascent CL and total MLCL (r = 0.955, P <0.0001), and a negative correlation between MLCL and *Tafazzin* expression (r = −0.593, P = 0.0883) were observed.

Conclusion: HCD modulated fatty acid compositions of CL and MLCL via *Tafazzin* in the liver, which could lead to mitochondrial dysfunction. This model may be useful for elucidating the relationship between fatty liver and mitochondrial dysfunction.

Introduction

Cardiolipin (CL) is a crucial phospholipid containing four fatty acyl chains and is located on the inner mitochondrial membrane.[1] Nascent CL is composed of various types of fatty acyls, and monolysocardiolipin (MLCL) is formed after one of fatty acyls constituting CL is enzymatically hydrolyzed. Finally, MLCL is transformed into the mature form of CL (tetralinoleoyl-CL; CL72:8) via remodeling.[2] CL72:8 is the most abundant CL[3] and regulates mitochondrial structure and respiration,[4] biogenesis, and energy production.[5]

Abnormal CL remodeling causes the depletion of mature CL, which could contribute to the pathophysiology of several metabolic diseases.[6] Reduction in CL levels have been associated with mitochondrial dysfunction, insulin resistance,[7] non-alcoholic fatty liver,[8] and liver injury.[9,10] Furthermore, a reduction in mitochondrial activation has been reported in patients with fatty liver.[9] In our recent study, we reported that hepatosteatosis, liver dysfunction, and abnormalities in the expression of primary proteins involved in mitochondrial function and lipogenesis were observed in overeating mice fed a high carbohydrate diet (HCD) for 5 days (short term) after 2 days of fasting.[11] Although the relationship between a carbohydrate-rich diet and changes in CL composition was determined in rats fed a high amounts of sucrose for a long-term period (24 weeks),[12] similar studies on the effect of such a diet for a short term have not been performed yet.

Abnormalities in CL remodeling may be accompanied by the changes in the expression of genes involved in CL remodeling and synthesis.[1,2] Nascent CL is synthesized by cardiolipin synthase (Cls) and hydrolyzed by calcium-independent phospholipase A2-γ (Pnpla8), resulting in the formation of MLCL. MLCL is then remodeled by *Tafazzin* (*Taz*) to form mature CL. In

71 another pathway, MLCL is remodeled by lysocardiolipin acyltransferase 1 (*Lclat1*), which
72 results in the formation of inactive CL (the other CL72:8). Notably, *Taz* plays an important role
73 in the biosynthesis of mature CL (CL72:8).

74 In this study, we aimed to determine the short-term effect of HCD on a mouse model of
75 fatty liver. We investigated whether such a diet administered even for a short term modulated CL
76 and MLCL levels in the mouse liver. We also performed gene expression analysis to elucidate
77 the underlying mechanism of the abnormalities introduced in CL remodeling, and modulation of
78 CL and MLCL levels.

Materials and Methods

Animal experiments

All animal experimental protocols were approved by the animal care committee of Hokkaido University (approval protocol number: 15-0174) as explained in a previous study.[11] In this study, we used the same liver samples as those reported in a previous study. [11] Briefly, nine male ddY mice (age: 7 week) were obtained from Sankyo Labo Service Corporation, Inc. (Sapporo, Japan) and housed individually with *ad libitum* access to solid-type food and water. Three mice comprising the control group were fed a normal chow diet (NCD) (Labo MR Stock, Nosan Corporation Life-Tech Department, Yokohama, Japan) without fasting. The NCD contained 3,291 kcal kg^{-1} (22.9% protein, 66.5% carbohydrate, 10.7% fat). In this study, untreated mice of the same age as the HCD group were used as control mice. On the other hands, six mice comprising the HCD group were fed a diet containing 380 g kg^{-1} sucrose for 5 days after fasting for 2 days to establish an overeating state that would lead to the development of acute fatty liver.[13] The HCD, which comprised 160 g kg^{-1} milk casein, 380 g kg^{-1} sucrose, 380 g kg^{-1} corn starch, 70 g kg^{-1} mineral mix, and 10 g kg^{-1} vitamin mix, was prepared from Hokudo Co. Ltd. (Sapporo, Japan)(See Supplemental Table 1) and contained 3,481 kcal kg^{-1} (15.9% protein, 82.8% carbohydrate, 1.3% fat). Three (control group) or six mice (experimental group) were compared to minimize the number of mice possible. The mice were anesthetized and sacrificed for collecting liver tissues that were stored at −80°C.

LC/MS analysis

Total lipids were extracted from the tissues by following the procedure described by Hara et al.[14] Briefly, the liver tissues were treated with 3:2 (v/v) hexane/isopropanol containing 20 μmol/mL butylated hydroxytoluene (Wako Pure Chemical, Osaka, Japan) twice. The extracts obtained were mixed and vacuum dried. The dried lipids were then dissolved in methanol (Wako Pure Chemical., Osaka, Japan), centrifuged at 15,000 rpm at 4°C for 15 min to remove any insoluble material, and stored at −80°C until further analysis.

LC/MS analysis was performed using a Shimadzu Prominence high-performance liquid chromatography system equipped with an LTQ Orbitrap mass spectrometer (Thermo-Fisher Scientific Inc., San Jose, CA) and an electrospray ionization (ESI) source, for which the major instrumental parameters were based on our previously reported protocol.[15] The obtained lipids were separated on an Atlantic T3 column (2.1 × 150 mm, 3 μm, Waters, Milford, MA). An LC gradient elution was performed by using a mobile phase consisting of 5 mM aqueous ammonium acetate, isopropanol, and methanol at a flow rate of 200 μL/min. For MS experiments, the following parameters were kept constant for the ESI negative mode: capillary voltage of −3.0 kV, capillary temperature of 330°C, sheath gas (nitrogen) flow of 50 arbitrary units, and auxiliary gas (nitrogen) flow of 5 auxiliary units. High-resolution MS data were obtained over a mass range of m/z 900–1650 in the Fourier transform mode with a resolving power of 60,000. MS/MS data were obtained in an ion-trap mode with an isolation width of 2.0 Da and an activation time of 30 ms. Tandem MS data were obtained using collision induced dissociation with a data-dependent mode including scans on the most intense ions, each of which were in the MS2 (collision energy of −35 V) and MS3 (collision energy of −45 V) spectra.

For all the data, each intensity was normalized by mg of wet liver used for the analysis. The raw data were processed using the workstation Xcalibur 2.2 (Thermo-Fisher Scientific Inc.), including peak annotation and peak area integration. The identification of lipid molecules was performed using the LIPIDMAPS database[16] and our in-house library,[15] as well as by comparing the LC retention behavior and MS fragment pattern with standards. The identified lipid molecular species were annotated as "class abbreviation + total carbon number in the fatty chain(s) + total double bond number in the fatty chain(s)."

The intensity of each analyte was calculated based on the peak area that was drawn using the extracted ion chromatogram with a tolerance of 5.0 ppm. For the elucidated CL types, the intensity of each fatty acyl could be calculated based on the equation given below:

$$Intensity_{Fatty\ acyl} = \sum (Intensity^{i}_{CL\ species} \times \frac{Fatty\ acyl\ quantity^{i}_{CL\ sepcies}}{4})$$

Real-time PCR

To analyze the expression of genes involved in the CL remodeling process, we performed real-time PCR. Total RNA was extracted from the liver tissues (20 mg wet) using PureLink® RNA Mini Kit (Thermo Fisher Scientific). The concentration and integrity of the isolated RNA were determined at $OD_{260/280}$ using a NanoDrop spectrophotometer (Thermo Fisher Scientific). The RNA was reverse-transcribed into cDNA using a ReverTra Ace qPCR RT Master Mix (Toyobo Co., Ltd., Osaka, Japan). Real-time PCR was performed using CFX 96 Real-Time PCR Detection System (Bio-Rad Laboratories Inc., Hercules, CA, USA) and

Thunderbird® SYBR qPCR Mix (Toyobo) according to the manufacturer's instructions. The sequences of primers used are given in Supplemental Table 2.[17,18] The PCR reaction was performed under the following conditions: 95°C for 60 s followed by 40 cycles at 95°C for 15 s and at 60°C for 30 s. The expression of all the genes was normalized to that of *Gapdh* in each sample. Data are represented as the relative expression to that in the NCD group.

Statistical analysis

Student's *t*-test was performed for comparing the data between the two groups. Two-way analysis of variance and the Tukey's multiple comparison test as a post-hoc test were performed and are shown in Figure 1B. All the data are shown as mean ± SD. Pearson's correlation coefficient was calculated to determine the relationship between total MLCL and total nascent CL levels or *Taz* expression in the liver. A *P*-value of <0.05 was considered as statistically significant. GraphPad Prism (version 7, GraphPad Software Inc., San Diego, CA, USA) was used for performing statistical analysis.

Results

Hepatic CL level

Thirty-two types of CL were identified in the liver (Figure 1A and Supplemental Table 3). In the NCD group, CL72:8 was the dominant type and constituted approximately 50% of all CLs. Total CL was calculated by adding the levels of all CLs detected in this study. Total CL level in the HCD group was 22% lower than that in the NCD group ($P < 0.05$) (Figure 1A, insert). The number of experimental mice was considered to be sufficient because the present results represented statistically significant differences between the groups.

In the HCD group, the proportion of CL72:8 in relation to total CL level was found to be strikingly decreased by 93% ($P < 0.0001$) (Figure 1B). We also calculated total nascent CL level (CLs other than CL72:8) by subtracting the CL72:8 level from the total CL level (Figure 1B). The nascent CL level was increased in the HCD group compared with that in the NCD group ($P < 0.01$). Nascent CL was the predominant CL type in the HCD group ($P < 0.0001$).

The fatty acyl profile of CL was different between the NCD and HCD groups (Figure 1C). The fatty acyl composition of CL revealed that FA18:2 was the predominant CL in the NCD group, whereas FA18:2 was less predominant in the HCD group.

3.2. Hepatic MLCL profile

Nine types of MLCL were identified in the liver (Figure 2). MLCL54:6, derived from CL72:8, was the most dominant type of CL in the NCD group. On the other hand, the level of MLCL54:6 was found to be insignificant in the HCD group ($P < 0.01$), whereas the levels of

178 other types were significantly higher in the HCD group than those in the NCD group. Total
179 MLCL level was calculated by adding all MLCL levels determined in this study and was 2.4-
180 fold higher in the HCD group than that in the NCD group (P <0.05) (Figure 2, insert).
181
182 **Gene expression analysis**
183 We analyzed the expression of genes involved in the CL remodeling process (Figure 3).
184 *Taz* expression was significantly downregulated in the HCD group compared with that in the
185 NCD group (P <0.05). *Lclat1* expression was also downregulated but it was not statistically
186 significant (P = 0.095). On the other hand, *Cls* expression was upregulated but it was not
187 statistically significant (P = 0.153). *Pnpla8* expression was similar between the two groups.
188
189 **Correlation between MLCL and nascent CL levels or *Taz* expression in the liver**
190 For determining the relationship between MLCL and nascent CL levels, we determined
191 the correlation coefficient (Figure 4). A strong positive correlation between the levels of nascent
192 CL (CLs other than mature CLs) and total MLCL was observed (r = 0.955, P <0.0001).
193 Similarly, we also determined the correlation coefficient of MLCL level and *Taz*
194 expression (Figure 4) and found a negative correlation between them (r = −0.593, P = 0.0883).
195

Discussion

To date, few studies have developed a mouse model for overeating-induced fatty liver in which changes in MLCL and CL levels are induced only after 5 days of administering an HCD. The results of our study were similar to a previous one in which downregulation of *Taz* expression and reduction in mature CL level were observed in the isolated mitochondria of rat fed with high amounts of sucrose for a long duration (24 weeks).[12] Thus, abnormal CL metabolism could be hampered because of unhealthy and irregular ways of eating even for a short period, thus indicating the effect of eating habits on human health.

We also reported that mitochondrial dysfunction could be caused by the low levels of several proteins involved in mitochondrial biogenesis, such as peroxisome proliferator-activated receptor gamma co-activator 1 alpha, mitochondrial thioredoxin, cardiolipin synthase, peroxisome proliferator-activated receptor alpha,[11] indicating that reduction in CL level and mitochondrial dysfunction could be directly related. CL is localized only in the mitochondrial cristae, and is strongly associated with regulating mitochondrial function.[19] Furthermore, hepatic CL level has been reported to be reduced in rats with non-alcoholic fatty liver,[8] which could result in mitochondrial dysfunction. Similar to these reports, a reduction in CL level was observed in the present mouse model of fatty liver (Figure 1A). Our mouse model could be useful in elucidating the underlying mechanism of the interaction between hepatic lipid droplets and the mitochondria in the future.

Figure 1 illustrates CL level modulation. Among the different types of CLs, CL72:8 possess the $(18:2)_4$ acyl chain and is considered to be a mature CL that plays a major functional

role in mammalian cells.[7,20-22] The $(18:2)_4$ acyl chain of CL is essential for its high affinity binding to proteins on the mitochondrial inner membrane. Hepatic CL72:8 level was lower in HCD group than in the NCD group.[23] In early type I and II diabetic mouse model, CL72:8 level in cardiomyocytes was found to be reduced probably because of abnormal CL remodeling .[24] Similarly, in the present study, hepatic CL72:8 level was markedly reduced, whereas MLCL level was increased (Figure 1B), clearly indicating abnormal CL remodeling in our mouse model.

CL remodeling enzymatically transfers the acyl group of phospholipids to MLCL, mainly via Tafazzin, followed by the production of mature CL. This regular remodeling plays an important role in maintaining mitochondrial function.[25] In another study, an increase in MLCL level caused by abnormal CL remodeling was attributed to mitochondrial dysfunction.[26] MLCL does not strongly interact with mitochondrial membrane proteins[27] but causes an inadequate production of electron transport chain-mediated ATP.[28] Interestingly, abnormality of CL remodeling seems to be correlated with the development of fatty liver. Them5-knockout mice developed not only fatty liver but also an increase in MLCL level.[29] *ALCAT-1* overexpression increased hepatic lipid droplets and abnormal CL remodeling.[30] A recent study reported that dietary fatty acids caused changes in hepatic mitochondrial CL levels and its fatty acid composition in rats with non-alcoholic fatty liver disease developed by administering a fat- and carbohydrate-rich diet for 8 weeks.[31] Since the phenotype associated with abnormal CL levels could be easily established in our model that included normal mice, we believe that our model

237 could help in better understanding of the pathology and onset of disorders associated with CL
238 remodeling.
239 *Tafazzin* is a phospholipid-lysophospholipid transacylase that transfers an acyl group
240 from phospholipids to MLCL, and is encoded by *Taz*, which is a critical gene for CL remodeling.
241 A previous study reported pathological changes in mitochondrial membranes in myofibrils,
242 skeletal muscles, and myocardium in *Taz*-deficient mice.[32] Mutations in *Taz* have been
243 associated with Barth syndrome, which is characterized by mitochondrial deficiency.[33]
244 Therefore, *Taz* downregulation could critically impair the biosynthetic pathway of mature CL.
245 On the other hand, an adeno-associated virus-mediated *Taz* replacement therapy by intravenous
246 injection can strikingly improve mitochondrial structure and function, heart function and
247 systemic activity level in the *Taz*-knockout mouse, which has been used as a mouse model of
248 Barth syndrome.[34] Perhaps therapeutics targeting *Taz* could be able to maintain normal CL and
249 MLCL levels and restore mitochondrial function. Thus, our mouse model might be useful for
250 demonstrating the effects of food extract, compounds, and drugs against mitochondrial
251 dysfunction via *Taz* expression.
252 In our study, levels of CLs except for CL72:8and MLCL were found to be increased
253 simultaneously. We believe that our study is the first to demonstrate a strong correlation between
254 CL72:8 and MLCL levels (Figure 4A). Similar to the increase in MLCL, an increase in nascent
255 CL level may lead to a reduction in mitochondrial function.[35] Our data suggest that an increase in
256 the precursors of mature CL is expected to cause mitochondrial dysfunction associated with
257 abnormal CL metabolism in the liver. Moreover, MLCL levels were found to be negatively

correlated with *Taz* expression in the liver (Figure 4), which is in accordance with the observation that *Taz* downregulation leads to increase in MLCL levels as reported in several previous studies.[36-38]

However, there are several limitations of this study. First, the reason for the downregulated expression of *Taz*, which was not observed for the other investigated genes, could not be ascertained in our proposed model. Thus far, the identity of the factors that control *Taz* expression upstream is unclear. Once they are identified, this issue may be resolved. Second, we attributed abnormal CL remodeling to mitochondrial dysfunction as previously mentioned.[4, 5, 6, 12, 25, 26, 28, 35] Therefore, in our future studies, we will focus on hepatic mitochondrial function directly to further elucidate the phenotype.

In conclusion, we found that HCD modulated fatty acyl compositions of CL and MLCL through Tafazzin in the liver, which could lead to mitochondrial dysfunction. Our mouse model of short-term overeating could be useful for elucidating the relationship between fatty liver and mitochondrial dysfunction in the future.

Author contributions

T.S., H.S., H.S., H.C., and S.P.H. designed the study. T.S., Z.C. and S.P.H performed lipidomics by LC/MS. T.H. performed the animal studies. T.S. and A.Y. performed hepatic gene expression analysis using real-time PCR. T.S., Z.C., A.Y., and H.C. wrote this manuscript. All authors have read and approved the final version of this manuscript.

Acknowledgements

A Grants-in-Aid for Regional R&D Proposal-Based Program from Northern Advancement Center for Science & Technology of Hokkaido, Japan, supported partially the present research. This study was supported by the Japanese Society for the Promotion of Science KAKENHI Grants (JP18K07434, JP19K07861, JP19K 2017409). This research was supported by Life Science Institute Co., Ltd. and Nissei Bio Co. Ltd. The Central Research Laboratory, Faculty of Health Sciences, Hokkaido University, provided us with the required work space.

Conflicts of interest

H. Satoh is employees of Nissei Bio Co., Ltd. H. Sekiguchi is employees of Life Science Institute Co., Ltd.

References

1 Chicco AJ and Sparagna GC, Role of cardiolipin alterations in mitochondrial dysfunction and disease. *Am J Physiol Cell Physiol* **292**:33–44 (2007).

2 Claypool SM and Koehler CM, The complexity of cardiolipin in health and disease. *Trends Biochem Sci* **37**:32–41 (2012).

3 Pennington ER, Funaib K, Brown DA and Shaik SR, The role of cardiolipin concentration and acyl chain composition on mitochondrial inner membrane molecular organization and function. *Biochim Biophys Acta Mol Cell Biol Lipids* **1864**:1039–1052 (2019).

4 Xu Y, Sutachan JJ, Plesken H, Kelley RI and Schlame M, Characterization of lymphoblast mitochondria from patients with Barth syndrome. *Lab Invest* **85**:823–830 (2005).

5 Song C, Zhang J, Qi S, Liu Z, Zhang X, Zheng Y *et al*., Cardiolipin remodeling by ALCAT1 links mitochondrial dysfunction to Parkinson's diseases. *Aging Cell* **18**:e12941 (2019).

6 Ye C, Shen Z and Greenberg ML, Cardiolipin remodeling: a regulatory hub for modulating cardiolipin metabolism and function. *J Bioenerg Biomembr* **48**:113–123 (2016).

7 Li J, Romestaing C, Han X, Li Y, Hao X, Wu Y *et al*., Cardiolipin remodeling by ALCAT1 links oxidative stress and mitochondrial dysfunction to obesity. *Cell Metab* **12**:154–165 (2010).

8 Petrosillo G, Portincasa P, Grattagliano I, Casanova G, Matera M, Ruggiero FM *et al*., Mitochondrial dysfunction in rat with nonalcoholic fatty liver involvement of complex I, reactive oxygen species and cardiolipin. *Biochim Biophys Acta Bioenerg* **1767**:1260–1267 (2007).

9 Pessayre D and Fromenty B, NASH: a mitochondrial disease. *J Hepatol* **42**:928– 940 (2005).

10 Labbe G, Pessayre D and Fromenty B, Drug-induced liver injury through mitochondrial dysfunction: mechanisms and detection during preclinical safety studies. *Fundam Clin Pharmacol* **22**:335–353 (2008).

11 Sakurai T, Hayasaka T, Sekiguchi H, Satoh H, Chen Z, Chiba H *et al*., Dietary salmon milt extracts attenuate hepatosteatosis and liver dysfunction in diet-induced fatty liver model. *J Sci Food Agric* **99**:1675–1681 (2019).

12 Ruiz-Ramírez A, Barrios-Maya MA, López-Acosta O, Molina-Ortiz D and El-Hafidi M, Cytochrome c release from rat liver mitochondria is compromised by increased saturated cardiolipin species induced by sucrose feeding. *Am J Physiol Endocrinol Metab* **309**:E777–786 (2015).

13 Delzenne NM, Hernaux NA and Taper HS, A new model of acute liver steatosis induced in rats by fasting followed by refeeding a high carbohydrate-fat free diet. Biochemical and morphological analysis. *J Hepatol* **26**:880–885 (1997).

14 Hara A and Radin NS, Lipid extraction of tissues with a low-toxicity solvent. *Anal Biochem* **90**:420–426 (1978).

15 Chen Z, Wu Y, Ma YS, Kobayashi Y, Zhao YY, Miura Y *et al*., Profiling of cardiolipins and their hydroperoxides in HepG2 cells by LC/MS. *Anal Bioanal Chem* **409**:5735–5745 (2017).

16 Sud M, Fahy E, Cotter D, Brown A, Dennis EA, Glass CK *et al*., LMSD: LIPID MAPS structure database. *Nucleic Acids Res* **35**:D527–532 (2007).

17 Acaz-Fonseca E, Ortiz-Rodriguez A, Lopez-Rodriguez AB, Garcia-Segura LM and Astiz M, Developmental sex differences in the metabolism of cardiolipin in mouse cerebral cortex mitochondria. *Sci Rep* **7**:43878 (2017).

18 Chen CC, Lee TY, Kwok CF, Hsu YP, Shih KC, Lin YJ *et al*., Cannabinoid receptor type 1 mediates high-fat diet-induced insulin resistance by increasing forkhead box O1 activity in a mouse model of obesity. *Int J Mol Med* **37**:743–754 (2016).

19 Paradies G, Paradies V, Ruggiero FM and Petrosillo G, Mitochondrial bioenergetics decay in aging: beneficial effect of melatonin. *Cell Mol Life Sci* **74**:3897–3911 (2017).

340 20 Pennington ER, Funai K, Brown DA and Shaikh SR, The role of cardiolipin concentration
341 and acyl chain composition on mitochondrial inner membrane molecular organization and
342 function. *Biochim Biophys Acta Mol Cell Biol Lipids* **1864**:1039–1052 (2019).
343 21 Semba RD, Moaddel R, Zhang P, Ramsden CE and Ferrucci L, Tetra-linoleoyl cardiolipin
344 depletion plays a major role in the pathogenesis of sarcopenia. *Med Hypotheses* **127**:142–149
345 (2019).
346 22 Pennington ER, Fix A, Sullivan EM, Brown DA, Kennedy A and Shaikh SR, Distinct
347 membrane properties are differentially influenced by cardiolipin content and acyl chain
348 composition in biomimetic membranes. *Biochim Biophys Acta Biomembr* **1859**:257–267
349 (2017).
350 23 Jha P, McDevitt MT, Gupta R, Quiros PM, Williams EG, Gariani K *et al*., Systems analyses
351 reveal physiological roles and genetic regulators of liver lipid species. *Cell Syst* **6**:722–773
352 (2018).
353 24 Han X, Yang J, Yang K, Zhao Z, Abendschein DR and Gross RW, Alterations in myocardial
354 cardiolipin content and composition occur at the very earliest stages of diabetes: a shotgun
355 lipidomics study. *Biochemistry* **46**:6417-6428 (2007).
356 25 Acehan D, Xu Y, Stokes DL and Schlame M, Comparison of lymphoblast mitochondria from
357 normal subjects and patients with Barth syndrome using electron microscopic tomography.
358 *Lab Invest* **87**:40–48 (2007).
359 26 Duncan AL, Monolysocardiolipin (MLCL) interactions with mitochondrial membrane
360 proteins. *Biochem Soc Trans* **48**:993–1004 (2020).

27 Xu Y, Phoon CKL, Berno B, DSouza K, Hoedt E, Zhang G *et al*., Loss of protein association causes cardiolipin degradation in Barth syndrome. *Nat Chem Biol* **12**:641–647 (2016).

28 Hoffmann B, Stöckl A, Schlame M, Beyer K and Klingenberg M, The reconstituted ADP/ATP carrier activity has an absolute requirement for cardiolipin as shown in cysteine mutants. *J Biol Chem* **269**:1940–1944 (1994).

29 Zhuravleva E, Gut H, Hynx D, Marcellin D, Bleck CKE, Genoud C *et al*., Acyl coenzyme A thioesterase Them5/Acot15 is involved in cardiolipin remodeling and fatty liver development. *Mol Cell Biol* **32**:2685–2697 (2012).

30 Wang L, Liu X, Nie J, Zhang J, Kimball SR, Zhang H *et al*., ALCAT1 controls mitochondrial etiology of fatty liver diseases, linking defective mitophagy to steatosis. *Hepatology* **61**:486–496 (2015).

31 Aoun M, Fouret G, Michel F, Bonafos B, Ramos J, Cristol J *et al*., Dietary fatty acids modulate liver mitochondrial cardiolipin content and its fatty acid composition in rats with nonalcoholic fatty liver disease. *J Bioenerg Biomembr* **44**:439–452 (2012).

32 Acehan D, Vaz F, Houtkooper RH, James J, Moore V, Tokunaga C *et al*., Cardiac and skeletal muscle defects in a mouse model of human Barth syndrome. *J Biol Chem* **286**:899–908 (2011).

33 Barth PG, Valianpour F, Bowen VM, Lam J, Duran M, Vaz FM *et al*., X-linked cardioskeletal myopathy and neutropenia (Barth syndrome): An update. *Am J Med Genet A* **126**:349–354 (2004).

34 Suzuki-Hatano S, Saha M, Rizzo SA, Witko RL, Gosiker BJ, Ramanathan M *et al*., AAV-mediated TAZ gene replacement restores mitochondrial and cardioskeletal function in Barth syndrome. *Hum Gene Ther* **30**:139–154 (2019).

35 Monteiro JP, Pereira CV, Silva AM, Maciel E, Baldeiras I, Peixoto F *et al*., Rapeseed oil-rich diet alters hepatic mitochondrial membrane lipid composition and disrupts bioenergetics. *Arch Toxicol* **87**:2151–2163 (2013).

36 Lou W, Reynolds CA, Li Y, Liu J, Hüttemann M, Schlame M *et al*., Loss of tafazzin results in decreased myoblast differentiation in C2C12 cells: A myoblast model of Barth syndrome and cardiolipin deficiency. *Biochim Biophys Acta* **1863**:857–865 (2018).

37 Valianpour F, Mitsakos V, Schlemmer D, Towbin JA, Taylor JM, Ekert PG *et al*., Monolysocardiolipins accumulate in Barth syndrome but do not lead to enhanced apoptosis. *J Lipid Res* **46**:1182–1195 (2005).

38 Richter-Dennerlein R, Korwitz A, Haag M, Tatsuta T, Dargazanli S, Baker M *et al*., DNAJC19, a mitochondrial cochaperone associated with cardiomyopathy, forms a complex with prohibitins to regulate cardiolipin remodeling. *Cell Metab* **20**:158–171 (2014).

Figure Legends

Figure 1. Analysis of cardiolipin level in liver tissues by LC/MS

(A) Cardiolipin (CL) levels in the liver. The insert is a figure indicating total CL level, which was calculated by adding the levels of all the CLs determined in this study. (B) Comparison of the levels of CL72:8 and other CLs (nascent CLs) between the two groups. (C) Summary of CL profile on the basis of each fatty acyl group. For all the data, each intensity was normalized by mg of wet liver used for analysis (NCD, n = 3; HCD, n = 6). * P <0.05, ** P <0.01, *** P <0.001, **** P <0.0001.

Figure 2. Distribution of monolysocardiolipin in the liver samples

MonolysoCL (MLCL) level in each group was simultaneously measured using LC/MS. For all the data, each intensity was normalized by mg of wet liver used for analysis (NCD, n = 3; HCD, n = 6). The insert is a figure illustrating total MLCL level, which was calculated by adding the levels of all MLCL determined in this study. * P <0.05, ** P <0.01, *** P <0.001 vs. the NCD group.

Figure 3. Effect on *Taz* expression in the high carbohydrate diet-fed group

Taz expression was analyzed by real-time PCR. The relative expression was normalized to that of *Gapdh*. * P <0.05, **** P <0.001 vs. the HCD group.

Figure 4. Correlation between total monolysocardiolipin and total nascent cardiolipin levels and *Taz* expression

(A) Pearson's correlation coefficient was calculated to determine the correlation between total monolysoCL (MLCL) and total nascent cardiolipin (CL) levels. (B) Pearson's correlation coefficient was calculated to determine the correlation between MLCL and *Taz* expression.

Figure 5. Hypothetical mechanism explaining mitochondrial dysfunction in the high carbohydrate diet-fed group

A high carbohydrate diet (HCD) fed for 5 days after 2 days of fasting lead to fatty liver development in our mouse model. It also caused altered the levels of cardiolipin (CL) and mono-lyso-CL (MLCL) in the liver. *Taz* downregulation could be involved in CL modulation. Thus, an increase in nascent CL (CL other than CL72:8) and MLCL levels as well as a decrease in mature CL (CL72:8) level via *Taz* downregulation may have resulted in mitochondrial dysfunction in the HCD group even in the short term. PC, phosphatidylcholine; LysoPC, lyso-phosphatidylcholine. PG, phosphatidylglycerol.

Figure 1.

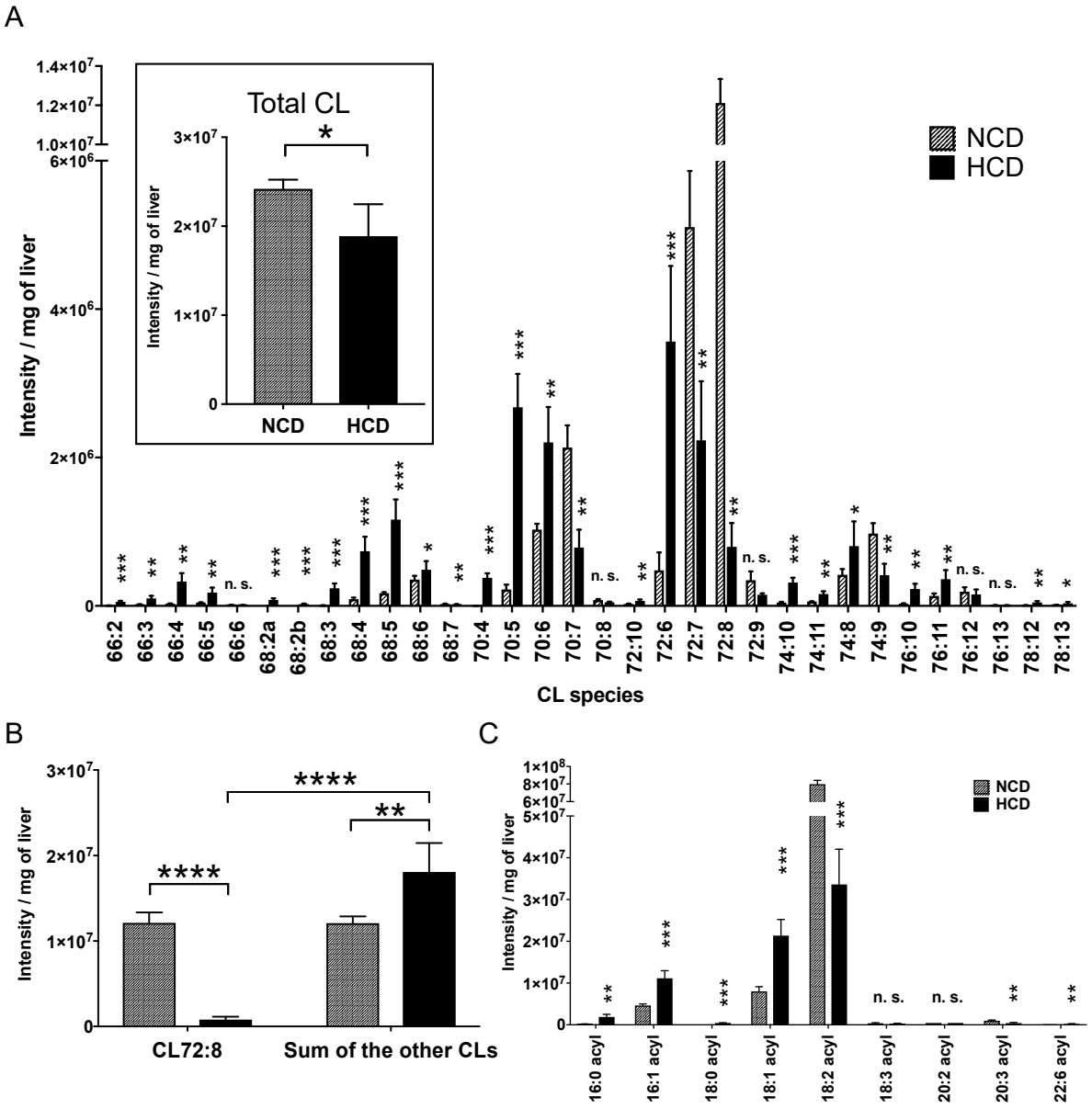
A
Total CL
Intensity / mg of liver
NCD
HCD
CL species
66:2
66:3
66:4
66:5
66:6
68:2a
68:2b
68:3
68:4
68:5
68:6
68:7
70:4
70:5
70:6
70:7
70:8
72:10
72:6
72:7
72:8
72:9
74:10
74:11
74:8
74:9
76:10
76:11
76:12
76:13
78:12
78:13
n. s.
B
CL72:8
Sum of the other CLs
C
16:0 acyl
16:1 acyl
18:0 acyl
18:1 acyl
18:2 acyl
18:3 acyl
20:2 acyl
20:3 acyl
22:6 acyl

Figure 2.

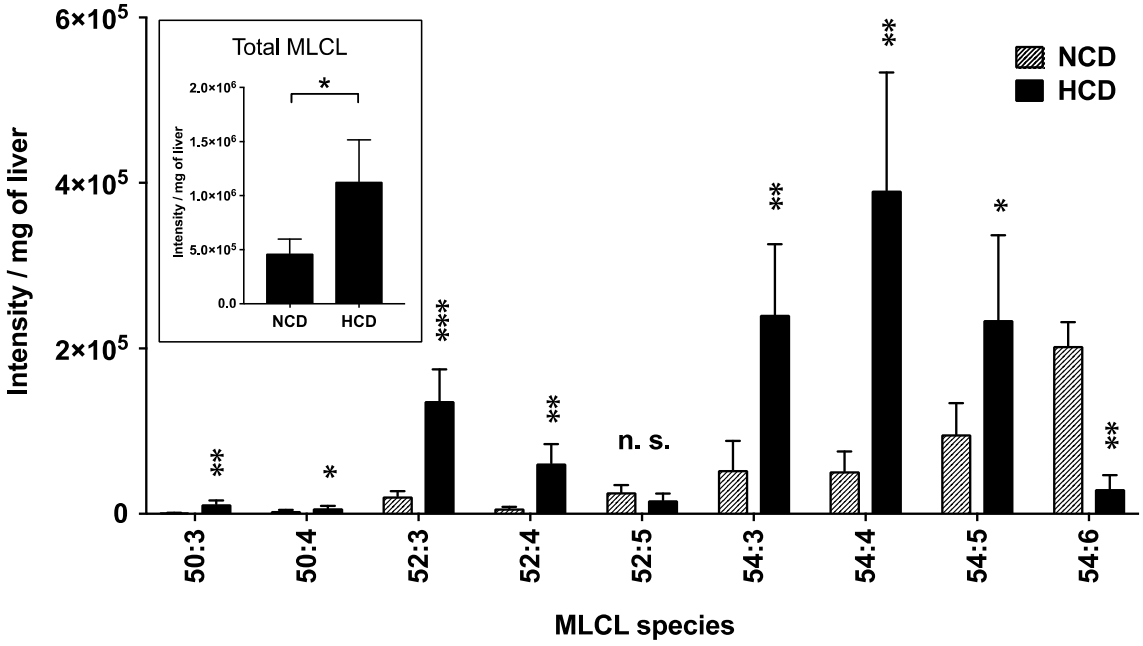
Total MLCL
Intensity / mg of liver
2.0×10^6
1.5×10^6
1.0×10^6
5.0×10^5
0.0
NCD
HCD
*
6×10^5
4×10^5
2×10^5
0
Intensity / mg of liver
NCD
HCD
**
*
***
**
n. s.
**
*
**
50:3
50:4
52:3
52:4
52:5
54:3
54:4
54:5
54:6
MLCL species

Figure 3.

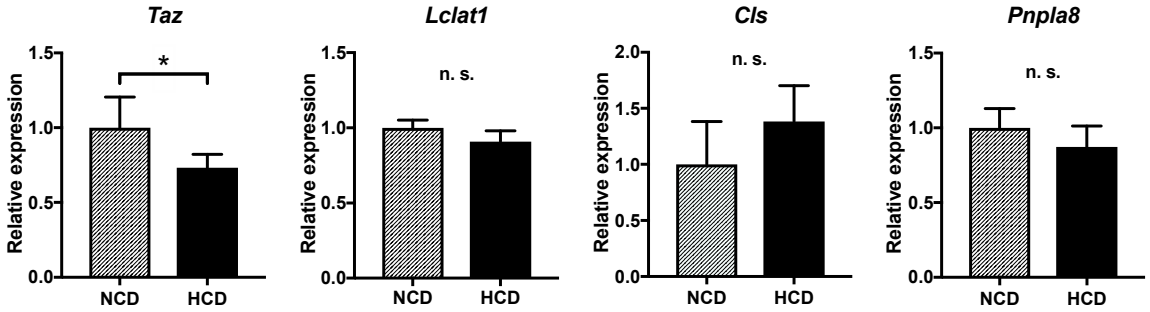
Taz
Lclat1
Cls
Pnpla8
Relative expression
1.5
1.0
0.5
0.0
2.0
1.5
*
n. s.
NCD
HCD

Figure 4.

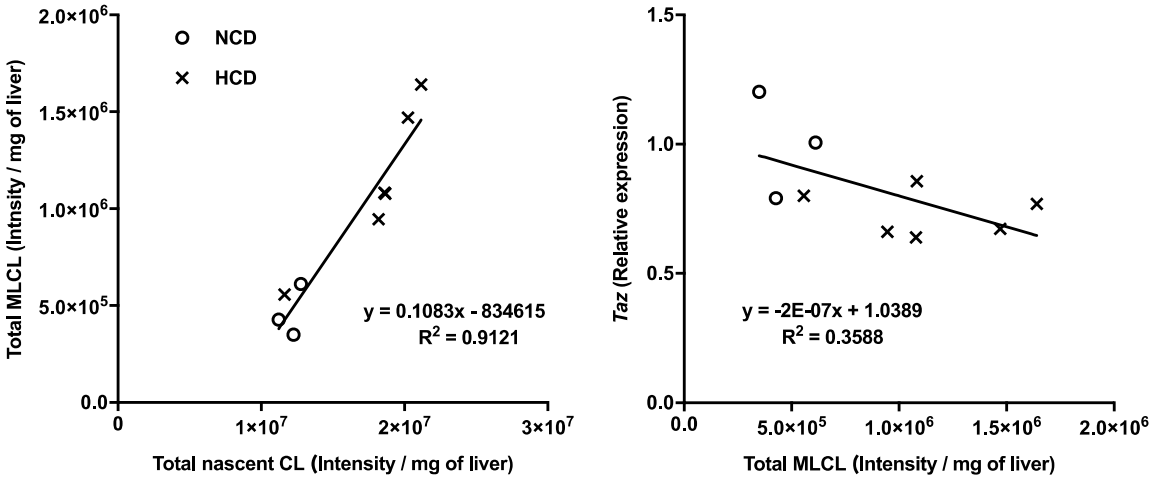
2.0×10^6
1.5×10^6
1.0×10^6
5.0×10^5
0.0
Total MLCL (Intnsity / mg of liver)
NCD
HCD
y = 0.1083x - 834615
R^2 = 0.9121
0
1×10^7
2×10^7
3×10^7
Total nascent CL (Intensity / mg of liver)
1.5
1.0
0.5
0.0
Taz (Relative expression)
y = -2E-07x + 1.0389
R^2 = 0.3588
0.0
5.0×10^5
1.0×10^6
1.5×10^6
2.0×10^6
Total MLCL (Intensity / mg of liver)

Figure 5.

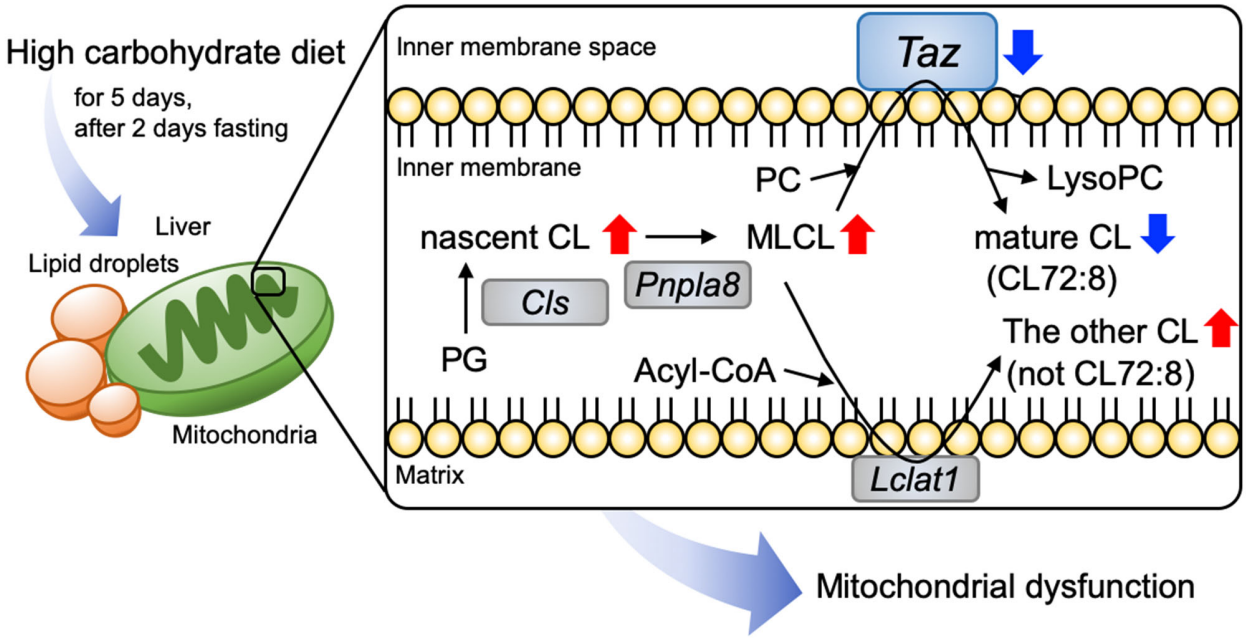
High carbohydrate diet
for 5 days,
after 2 days fasting
Liver
Lipid droplets
Mitochondria
Inner membrane space
Taz
Inner membrane
PC
LysoPC
nascent CL
MLCL
mature CL
(CL72:8)
Cls
Pnpla8
PG
Acyl-CoA
The other CL
(not CL72:8)
Matrix
Lclat1
Mitochondrial dysfunction

Supplemental Table1. Diet composition of HCD

	g kg^{-1}
Milk casein	160
Sucrose	380
Corn starch	380
Mineralmix	70
Vitamin mix	10

The special diet, high carbohydrate diet (HCD), was prepared from Hokudo Co. Ltd. (Sapporo, Japan).

Supplemental Table 2. Primer sequences for real-time PCR

Genes	Forward (5'-3')	Reverse (5'-3')	Ref.
Taz	CCTGAAGTTGATGCGTTGGA	GACACACAGGCACACATTTGC	17
Lclat1	GCATTTGTTAGTGGGAGAGTGCTA	GTAAGTTCCCAGCAGGATTAAAGTG	17
Cls	TGTAATGTTGATCGCTGCTGTGT	CCTAGCCGTGGCATAGCAA	17
Pnpla8	GGAATAGAAGTGAAGCACATTGCA	TAAGTCCCTTGGGAGCAGAAGT	17
Gapdh	TCACCACCATGGAGAAGGC	GCTAAGCAGTTGGTGGTGCA	18

Supplemental table 3. Identification of detected CL species

CL species	Calc. *m/z*	Tested *m/z*	Δppm	Fatty acyl composition
CL66:2	1375.9649	1375.9636	-0.94	N/A
CL66:3	1373.9493	1373.9523	2.18	N/A
CL66:4	1371.9336	1371.9348	0.87	16:1/18:1/16:1/16:1
CL66:5	1369.9180	1369.9188	0.58	16:1/18:2/16:1/16:1
CL66:6	1367.9023	1367.9020	-0.22	N/A
CL68:2a	1403.9962	1403.9960	-0.14	16:0/18:1/18:0/16:1
CL68:2b	1403.9962	1403.9977	1.07	16:0/18:1/18:1/16:0
CL68:3	1401.9806	1401.9830	1.71	16:1/18:1/18:1/16:0
CL68:4	1399.9649	1399.9672	1.64	16:1/18:1/18:1/16:1
CL68:5	1397.9493	1397.9509	1.14	16:1/18:2/18:1/16:1
CL68:6	1395.9336	1395.9338	0.14	16:1/18:2/18:2/16:1
CL68:7	1393.9180	1393.9186	0.43	N/A
CL70:4	1427.9962	1427.9976	0.98	16:1/18:1/18:2/18:0
CL70:5	1425.9806	1425.9814	0.56	16:1/18:1/18:2/18:1
CL70:6	1423.9649	1423.9648	-0.07	16:1/18:2/18:2/18:1
CL70:7	1421.9493	1421.9491	-0.14	16:1/18:2/18:2/18:2
CL70:8	1419.9336	1419.9309	-1.90	N/A
CL72:6	1451.9962	1451.9968	0.41	18:1/18:2/18:2/18:1
CL72:7	1449.9806	1449.9813	0.48	18:1/18:2/18:2/18:2
CL72:8	1447.9649	1447.9637	-0.83	18:2/18:2/18:2/18:2
CL72:9	1445.9493	1445.9442	-3.53	18:2/18:3/18:2/18:2
CL72:10	1443.9336	1443.9338	0.14	18:2/18:3/18:3/18:2
CL74:8	1475.9962	1475.9944	-1.22	18:2/20:2/18:2/18:2
CL74:9	1473.9806	1473.9790	-1.09	18:2/20:3/18:2/18:2
CL74:10	1471.9649	1471.9628	-1.43	N/A
CL74:11	1469.9493	1469.9478	-1.02	N/A
CL76:10	1499.9962	1499.9941	-1.40	18:1/22:6/18:2/18:1
CL76:11	1497.9806	1497.9777	-1.94	N/A
CL76:12	1495.9649	1495.9620	-1.94	N/A
CL76:13	1493.9493	1493.9495	0.13	N/A
CL78:12	1523.9962	1523.9906	-3.67	N/A
CL78:13	1521.9806	1521.9790	-1.05	N/A

N/A: Not available.